New Phytologist

Research

Rapid report

The geometry of the compound leaf plays a significant role in the leaf movement of *Medicago truncatula* modulated by *mtdwarf4a*

Authors for correspondence:
Liangliang He
Email: heliangliang@xtbg.ac.cn

Jianghua Chen
Email: jhchen@xtbg.ac.cn

Received: *21 July 2020*
Accepted: *9 January 2021*

Weiyue Zhao[1,2], Quanzi Bai[1,2], Baolin Zhao[1], Qing Wu[1,2], Chaoqun Wang[1,2], Ye Liu[1,3], Tianquan Yang[1,4], Yu Liu[1], Hua He[1], Shanshan Du[1,2], Million Tadege[5], Liangliang He[1] and Jianghua Chen[1,2,3]

[1]CAS Key Laboratory of Tropical Plant Resources and Sustainable Use, CAS Center for Excellence in Molecular Plant Sciences, Xishuangbanna Tropical Botanical Garden, Chinese Academy of Sciences, 88 Xuefu Road, Kunming, Yunnan 650223, China; [2]University of Chinese Academy of Sciences, Beijing 100049, China; [3]School of Life Sciences, University of Science and Technology of China, Hefei, Anhui 230027, China; [4]Germplasm Bank of Wild Species, Kunming Institute of Botany, Chinese Academy of Sciences, Kunming 650201, China; [5]Department of Plant and Soil Sciences, Institute for Agricultural Biosciences, Oklahoma State University, 3210 Sam Noble Parkway, Ardmore, OK 73401, USA

New Phytologist (2021) **230:** 475–484
doi: 10.1111/nph.17198

Key words: brassinosteroid (BR) biosynthesis, compound leaf geometry, *DWARF4*, leaf movement, *Medicago truncatula*, pulvinus.

Summary

- In most legumes, two typical features found in leaves are diverse compound forms and the pulvinus-driven nyctinastic movement. Many genes have been identified for leaf-shape determination, but the underlying nature of leaf movement as well as its association with the compound form remains largely unknown.
- Using forward-genetic screening and whole-genome resequencing, we found that two allelic mutants of *Medicago truncatula* with unclosed leaflets at night were impaired in *MtDWARF4A* (*MtDWF4A*), a gene encoding a cytochrome P450 protein orthologous to *Arabidopsis* DWARF4.
- The *mtdwf4a* mutant also had a mild brassinosteroid (BR)-deficient phenotype bearing pulvini without significant deficiency in organ identity. Both *mtdwf4a* and *dwf4* could be fully rescued by *MtDWF4A*, and *mtdwf4a* could close their leaflets at night after the application of exogenous 24-epi-BL. Surgical experiments and genetic analysis of double mutants revealed that the failure to exhibit leaf movement in *mtdwf4a* is a consequence of the physical obstruction of the overlapping leaflet laminae, suggesting a proper geometry of leaflets is important for their movement in *M. truncatula*.
- These observations provide a novel insight into the nyctinastic movement of compound leaves, shedding light on the importance of open space for organ movements in plants.

Introduction

The pulvinus-driven nyctinastic leaf movement, a common and characteristic phenomenon found in the Leguminosae (Fabaceae) and Oxalidaceae, has intrigued plant scientists and the public since Darwin's era (Darwin & Darwin, 1881). Most species from both taxa have compound leaves with multiple joined units termed leaflets, and the geometry of leaflets (the spatial structure and organization of leaflets) largely determines the compound leaf shape, which has been broadly recognized in model compound-leafed species (Scarpella *et al.*, 2010; Runions *et al.*, 2017). Each leaflet usually has an independent pulvinus at the base of the lamina, functioning as the motor organ for leaf movement. Two functionally and positionally antagonistic groups of motor cells exist in the pulvinus, known as the extensor and flexor, and leaflet movements are generated by changes in turgor pressure of these motor cells (Satter & Galston, 1971; Racusen & Satter, 1975; Gorton & Satter, 1984; Cote, 1995; Moshelion *et al.*, 2002a,b). Chloride ion (Cl^-) and potassium ion (K^+) channels play key roles in the regulation of turgor pressure in motor cells, and molecular evidences have recently been reported in *Samanea saman* (Oikawa *et al.*, 2018; Ueda *et al.*, 2019). The determination of pulvinus

identity in legumes seemingly shares a conserved genetic network orchestrated by a plant specific LOB DOMAIN-CONTAINING PROTEIN (LBD) transcription factor, namely SLEEPLESS (SLP) in *Lotus japonicas*, APULVINIC (APU) in pea (*Pisum sativum*) and ELONGATED PETIOLULE1 (ELP1)/PETIOLULE-LIKE PULVINUS (PLP) in *Medicago truncatula* (Harvey, 1979; Kawaguchi, 2003; Chen *et al.*, 2012; Zhou *et al.*, 2012). The identification of the APC8-like protein *Glycine max* Increased Leaf Petiole Angle1 (GmILPA1) revealed that the number and size of motor cells of pulvinus are also important for the pulvinus function (Gao *et al.*, 2017). The previous studies mainly focused on the role of the pulvinus in leaf movement, but to date, there is very little information about the contribution of other elements of the compound leaf, e.g. the leaflet geometry, to the movement phenomenon.

Medicago truncatula, with trifoliate leaves characterized by the opening of leaflets near dawn and their closing near dusk following a circadian rhythm, has become a key model to investigate the mechanisms of leaf movement as well as of compound leaf pattern formation (Wang *et al.*, 2008; Chen *et al.*, 2010, 2012; Young *et al.*, 2012). Several key genes have been shown to regulate leaflet development and organization in the compound leaf of *M. truncatula* (Zhao *et al.*, 2020; He *et al.*, 2020), but the underlying molecular mechanism of its nyctinastic leaf movement is just beginning to be unraveled, opening new doors for further mechanistic dissection (Chen *et al.*, 2012; Kong *et al.*, 2020).

In this study, two allelic mutants that cannot close their leaflets during the night in contrast to the wild type (WT) were identified through forward genetic screening and molecularly characterized. A combination of whole genome sequencing, genetic linkage and complementation analyses revealed that these mutants are loss-of-function *mtdwarf4a* (*mtdwf4a*) alleles. The pulvinus structure and identity is slightly affected in *mtdwf4a*, whereas surgical experiments and genetic analysis of double mutants indicated that the overlapping leaflet laminae in *mtdwf4a* compound leaves present a barrier to the leaflet movement. The study revealed that the inability to exhibit leaf movement in *mtdwf4a* is mainly a consequence of the physical obstruction of the overlapping leaflet laminae. This provided us with a novel insight into the compound leaf movement in *M. truncatula*, that the open space between leaflets in a compound leaf is necessary for leaflets to close at night.

Materials and Methods

Plant materials and growth conditions

The *mtdwf4a* mutants of *M. truncatula* were isolated through forward-genetic screening from a tobacco *Tnt1* retrotransposon tagged mutant collections as previously reported (d'Erfurth *et al.*, 2003; Tadege *et al.*, 2008). Seeds of Col-0 (WT) and *dwf4-96* (SAIL_580_B09) were ordered from Arabidopsis Biological Resource Center (ABRC, Columbus, OH, USA). *Arabidopsis* seeds were surface-sterilized and placed in the soil or on the half strength Murashige and Skoog (½MS) medium supplemented with 50 mg l^{-1} kanamycin for screening the positive transgenic plants. Plants were grown in glasshouses under the following conditions: 22°C with 15 h : 9 h, light : dark photoperiod, 150 µmol m^{-2} s^{-1} light intensity and 50% to 60% relative humidity.

Whole genome resequencing

The F_2 population was derived from backcrossing *mtdwf4a-1* and the WT (R108). Equal weight of leaves from 10 F_2 homozygous *mtdwf4a-1* mutants were collected and mixed to extract DNA using a HiPure Plant DNA Mini Kit following the manufacturer's instructions (Magen , Guangzhou, China). This DNA sample was used for genome resequencing at 20× coverage. The resequencing data was analyzed by the bioinformatics tool, Identification of Transposon Insertion Sites (ITIS) (Jiang *et al.*, 2015), which has been successfully applied to *M. truncatula* previously (Zhao *et al.*, 2020; Zheng *et al.*, 2020).

RNA extraction, RT-PCR and real-time PCR (RT-qPCR) analyses

Total RNA of different tissues from 1-month-old plants were extracted using TransZol (TransGen, Beijing, China). Complementary DNA (cDNA) synthesis was carried out with 2 µg of total RNA using the TransScript II One-Step gDNA Removal kit (Takara, Shiga, Japan). Reverse transcription quantitative polymerase chain reaction (RT-qPCR) was performed using TransStart Tip Green qPCR SuperMix (TransGen) on a LightCylcer 480 device (Roche, Basel, Switzerland). Primer sequences are listed in Supporting Information Table S1.

Genetic complementation

Full-length coding sequence of *MtDWF4A* (1452 bp, R108) was amplified by PCR with Phanta MaxSuper-Fidelity DNA Polymerase (Vazyme, Nanjing, China), and then constructed into final vectors and named as *pCAMBIA3301-35S::MtDWF4A* (for *mtdwf4a-1*), *pPYS22-35S::AtDWF4* and *pPYS22-35S::MtDWF4A* (for *dwf4-96*) by ClonExpress II One Step Cloning Kit (Vazyme). *Agrobacterium tumefaciens* EHA105 strains with those two constructs described earlier were used for the respective genetic transformation of *M. truncatula* and *Arabidopsis* mutants as previously described (Clough & Bent, 1998; Chabaud *et al.*, 2007; Du *et al.*, 2016). Primer sequences are listed in Table S1.

Semi-thin sections

Histological slide preparation followed Feder & Obrien (1968). Pulvini from WT and mutants were fixed in the formalin-aceto-alcohol (FAA) solution before alcohol gradient dehydration and glycol methacrylate (GMA) penetration. Semi-thin sections were performed on a Leica UC7 and visualized with an Olympus BX63 microscope as recently reported (Zheng *et al.*, 2020). Histology characteristics of pulvini were examined using 0.05% toluidine blue staining for 5 s.

Scanning electron microscopy (SEM) analysis and photography

Scanning electron microscopy (SEM) analysis followed Wang *et al.* (2008). Specimens were examined under a Sigma 300 microscope (Zeiss, Oberkochen, Germany) at an accelerating voltage of 5 kV. Digital photographs were taken with a Nikon D7100 camera or the light stereomicroscopy (SZX16; Olympus), and then assembled using Adobe PHOTOSHOP CS5.

RNA *in situ* hybridization

Shoot apices of 3-wk-old plants were collected for RNA *in situ* hybridization as previously described (Coen *et al.*, 1990). The PCR product of full-length *MtDWF4A* CDS was labeled with digoxigenin to generate probes.

Phylogenetic analysis

Phylogenetic analysis was performed as described before (He *et al.*, 2020). Alignment of multiple sequences was performed by CLUSTAL X2 (Thompson *et al.*, 1997). Phylogenetic tree was constructed using IQTREE v.1.6.10 and edited with MEGA5.1 software (Tamura *et al.*, 2007).

BR measurement and 24-epi-BL treatment

The shoot apical tissues containing developing leaves from 1-month-old WT and *mtdwf4a-1* plants grown on ½MS media were harvested and weighed (no < 100 mg containing 50–70 individuals for one independent sample). Brassinosteroid (BR) contents were determined by the Wuhan Greensword Creation Technology Co. Ltd (http://www.greenswordcreation.com) using high-performance liquid chromatography tandem mass spectrometry (HPLC-MS/MS) as described previously with minor modification (Ding *et al.*, 2013). For exogenous application of BRs, about 10 ml of 1 μM 24-epi-brassinolide (BL) solution was sprayed on a total of 10 plants (five WT and five *mtdwf4a-1*) one time. Plants were first sprayed at 1 wk after germination in soil, with daily sprays continuing for 2 wk. Compound leaves of the third internode beneath the shoot apex were photographed at 10 d after the sprays were stopped.

Surgical experiment

All surgical experiments were performed on compound leaves of the third internode beneath the shoot apex of 4- to 6-wk-old plants, and photographs were taken at 2 d after surgical treatment.

Results

Isolation and characterization of the *mtdwf4a* mutant in *M. truncatula*

To gain a better understanding of nyctinastic leaf movement in legumes, we performed a large-scale forward genetic screening in *Tnt1* retrotransposon-tagged mutant populations of the model legume *M. truncatula* (Cultivar (cv.) R108). The three leaflets in WT leaves are flattened in the day and folded toward the petiole at night (Fig. 1a–e, left). Two mutant lines with similar leaf movement phenotypes being unable to fold theirs leaflets in night were isolated (Fig. 1a–e, right). An allelism test demonstrated that the two mutant lines were allelic to each other (Supporting Information Fig. S1) and temporarily designated as *leaflet movement1-1* (*lm1-1*) and *lm1-2* (later also called '*mtdwf4a-1*' and '*mtdwf4a-2*', which names are used in all figures). The F_1 plants derived from a backcross of *lm1-1/mtdwf4a-1* with WT (cv. R108) exhibited a WT phenotype. The F2 progenies from self-pollination of the F_1 plants showed a segregation of WT and mutant types at a ratio of 3 : 1, indicating that the *lm1-1/mtdwf4a-1* mutant was caused by a single recessive nuclear gene mutation.

The mature leaflets of *lm1-1/mtdwf4a-1* were epinastic with wavy lamina and reduced marginal projections (Fig. 1c,d, right), significantly different from the flattened leaflets of WT (Fig. 1c,d, left). In WT trifoliate leaves, the central rachis plays an important role in sculpting the space between the terminal leaflet (TL) and the pair of lateral leaflets (LLs), and thus is crucial to the trifoliate leaf geometry, while the two LLs are connected to the petiole through their pulvini, which is therefore advantageous for ensuring the space between the two LLs (Fig. 1c,d, left). The *lm1-1/mtdwf4a-1* mutant had the shortened rachis and pulvini (Fig. 1f,h), causing the three leaflet laminae to partially overlap with each other and the space between three leaflets being extremely crowded (Fig. 1c, right). In addition, the petiole length and plant height of *lm1-1/mtdwf4a-1* were significantly reduced compared with those of WT (Fig. 1g,i).

Images taken with SEM showed that the surface identity of the epidermal cells of the *lm1-1/mtdwf4a-1* pulvini was WT-like, with the exception that the cell length was slightly diminished (Fig. 1j,k). Anatomical studies of transverse sections indicated that structure and cell morphology of the pulvini of *lm1-1/mtdwf4a-1* were remarkably similar to those of WT, with the central vascular bundle surrounded by outer circled motor cells (Fig. 1l,m). These results revealed that the pulvinus structure of *lm1-1/mtdwf4a-1* was very similar to that of WT, with slight differences in size and cell organization.

Taken together, the *lm1-1/mtdwf4a-1* mutant differed marginally from the WT with respect to the pulvinus structure but possessed strikingly altered geometry of the compound leaves.

Molecular cloning and genetic complementation analysis

To clone the gene responsible for the *lm1* mutant phenotype, 10 *lm1-1* mutants from a BC_2F_2 population developed from the *lm1-1* × WT (cv. R108) cross were collected and processed for whole genome re-sequencing at 20× coverage. Then, the sequence data were analyzed by the bioinformatics tool, ITIS, as previously described (Jiang *et al.*, 2015; Zhao *et al*, 2020; Zheng *et al.*, 2020). ITIS identified seven homozygous *Tnt1* insertions in the genome of *lm1-1*, and four of them were inserted into genic regions (Table S2). The expression profiles of the four candidate genes were obtained in the network (https://mtgea.noble.org/v3/blast_

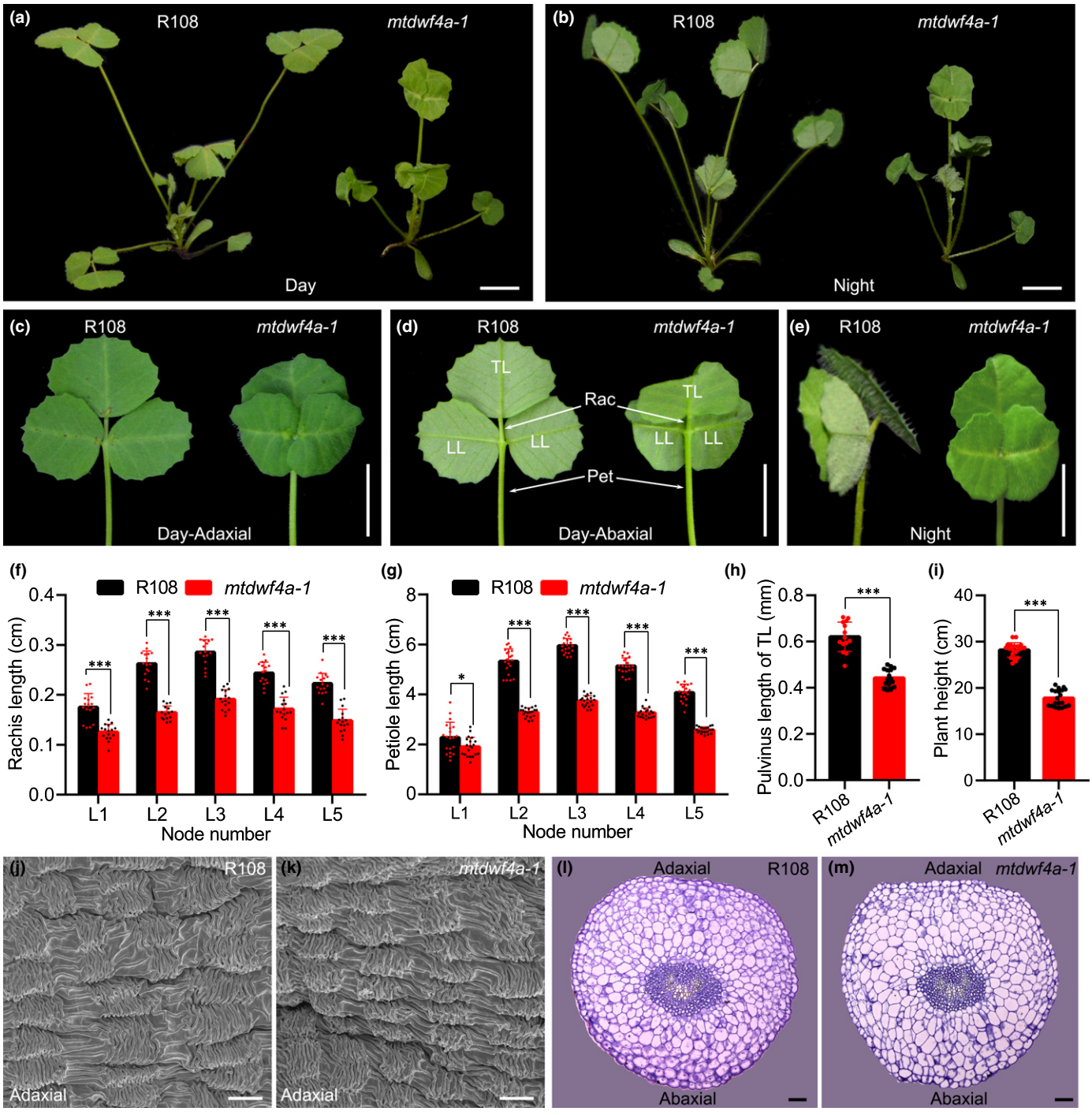

Fig. 1 The *mtdwf4a-1* mutant of *Medicago truncatula* has pleiotropic phenotypes. (a, b) The leaf movement phenotype of 1-month-old wild-type (WT) cv R108 (a, left) and *mtdwf4a-1* mutant (a, right) during daytime, WT plant (b, left) and *mtdwf4a-1* mutant (b, right) during nighttime. (c, d) Morphologies of adaxial (c) and abaxial surface (d) of the adult leaves of WT (left) and *mtdwf4a-1* mutant (right) during daytime. TL, terminal leaflet; LL, lateral leaflet; Rac, rachis; Pet, petiole. (e) Close-up views of leaflets in WT (left) and *mtdwf4a-1* (right) mutant during nighttime. (a–e; bars, 1 cm). (f–g) The length of rachis (f) and petiole (g) in 1-month-old WT and *mtdwf4a-1* plants ($n = 15$). (h) Pulvinus length of the TL in WT and *mtdwf4a-1* (compound leaves of the third internode beneath the shoot apex from 1-month-old plants were counted, $n = 10$). (i) The height of 2-month-old WT and *mtdwf4a-1* plants ($n = 20$). Values in (f–i) shown in the form of mean ± SD, and asterisks indicate a statistically significant difference between WT and *mtdwf4a-1* (*, $P < 0.05$; ***, $P < 0.001$; unpaired two-sample *t*-test). (j–m) SEMs (bars, 10 μm) and semi-thin transverse sections (bars, 50 μm) of the TL pulvini of the third internode leaves beneath the shoot apex of 1-month-old WT (j, l) and *mtdwf4a-1* plants (k, m).

search_form.php) (Fig. S2). PCR-based genotyping found that a genic region corresponding to the *MtDWARF4A* (*MtDWF4A*; gene ID *Medtr5g020020* in version Mt4.0v1) contained homozygous *Tnt1* insertions in both *lm1-1* and *lm1-2* (hereafter renamed as *mtdwf4a-1* and *mtdwf4a-2*) mutant lines (Fig. S3a–c). Co-segregation analysis in the backcrossed F_2 populations of the

mtdwf4a-1 and *mtdwf4a-2* mutant lines showed that all individual mutants were homozygous for their *Tnt1* insertions in *MtDWF4A* (Fig. S3b,c). In addition, we performed a reverse genetic screening via BLAST searching against the public mutant-database (https://medicago-mutant.noble.org/mutant/) and isolated another two alleles *mtdwf4a-3* and *mtdwf4a-4* that harbored predicted *Tnt1* insertions at the *MtDWF4A* gene (Fig. 2a; Table S3). Individuals with homozygous *Tnt1* insertions of both *mtdwf4a-3* and *mtdwf4a-4* lines resembled the phenotypes of *mtdwf4a-1* and *mtdwf4a-2* (Fig. S4). RT-PCR results confirmed that all the *mtdwf4a* mutant lines were real knock-out alleles of the *MtDWF4A* gene (Fig. S3d).

For complementation test, we introduced the *35S::MtDWF4A* construct into the *mtdwf4a-1* mutants using *Agrobacterium tumefaciens*-mediated stable transformation and eventually generated seven independent transgenic lines. Phenotypic and RT-qPCR analyses indicated that the expression of *MtDWF4A* completely rescued the morphological defects and leaf movement ability of the *mtdwf4a-1* mutants (Fig. 2b–h). These data provided the direct and solid evidence to support that the loss-of-function mutation of *MtDWF4A* was responsible for the defective phenotypes of the *mtdwf4a* mutants.

Phylogenetic analysis and the expression pattern of *MtDWF4A*

Phylogenetic analysis revealed that *MtDWF4A* encodes a cytochrome P450 protein homologous to the *Arabidopsis* BR biosynthetic enzyme DWF4 (Choe *et al.*, 1998) and grouped into the well-supported DWF4 clade (Fig. 3a). Almost all legume species (except *L. japonicus*) have at least two copies in the DWF4 clade, with one very close copy (designated as *MtDWARF4B*; gene ID *Medtr8g077810*) of *MtDWF4A* found in the *M. truncatula* genome (Fig. 3a). MtDWF4A shows a high degree of amino acid sequence similarity with DWF4 and another important BR biosynthetic enzyme, constitutive photomorphogenesis and dwarfism (CPD) from *Arabidopsis* (Fig. S5). The heterogenous complementation test in *Arabidopsis* showed a functional equivalence between *MtDWF4A* and *AtDWF4*, because *35S::MtDWF4A* could completely restore the defective phenotypes of *dwf4-96*, a weak loss-of-function mutant allele of *DWF4*, and some transgenic plants showing phenotypes of elongated petioles and leaf blades were similar to the plants overexpressing the BR biosynthetic enzyme or BR receptor (Choe *et al.*, 2001; Wang *et al.*, 2001; Du *et al.*, 2016; Bajguz *et al.*, 2020) (Figs 3b, S6). Hormone measurement showed that endogenous bioactive BR content was significantly decreased in *mtdwf4a-1* (Fig. S7). Subsequent application of exogenous 24-epi-BL effectively restored the compound leaf shape defects in *mtdwf4a-1*, leading to the recovery of leaflet movement (Fig. 3c). These results indicate that the BR biosynthetic pathway was affected in the mutant and *MtDWF4A* plays a conserved function in BR biosynthetic pathway.

Similar to the *AtDWF4*, the transcript of *MtDWF4A* was widely detected in different tissues with highest expression level in the leaves (Fig. 3d). The RNA *in situ* hybridization assay showed that the transcript of *MtDWF4A* was detected at the basal region of the TL and LL primordia at early stages of leaf development (Fig. 3e). At later leaf developmental stages, *MtDWF4A* transcripts were clearly detected in different regions of leaf primordia, including blade, rachis and petiole. This expression pattern essentially coincides with the tissue where the defects occurred.

Surgical experiments and genetic interactions between *mtdwf4a* and leaf geometry mutants

Since the pulvini of *mtdwf4a-1* appeared to be of normal structure and identity, we wondered whether the changed geometry of *mtdwf4a-1* compound leaves contributed to the failure to exhibit movement behavior. To verify this, at first, the overlapping tissues between the leaflets of *mtdwf4a-1* were cut off without damaging any structure of pulvini, while equivalent tissues in WT leaves were also tailored (Fig. 4a). As shown in Fig. 4(d), in the untreated control group, the angle between the two LLs of WT was close to 0° at Zeitgeber time (ZT) 19.5 (4.5 h after lights off), while the angle between the LLs of *mtdwf4a-1* was almost 180° throughout the day. The surgical experiments showed no influences on the normal nyctinastic movement of WT plants (Fig. 4b–d). However, after removing the physically overlapping parts of laminae, the leaflets of *mtdwf4a-1* came remarkably close during night despite having a lower degree than that of WT (Fig. 4b–d). For comparison, some surgical experiments avoiding the overlapping parts failed to restore the leaflet movement (Fig. S8). Taken together, these observations suggest that the inability to close leaflets at night in *mtdwf4a-1* is mainly because of the crowding of spaces between leaflets which caused physical obstruction between leaflets when the movement occurred. This conclusion is further supported by the facts that both the first unifoliate leaf and the remaining TL part of compound leaf after removing the two LLs could incline to the petiole during night in *mtdwf4a-1* (Fig. S9).

Next, the *mtdwf4a-1* mutant was crossed with the *stenofolia* (*stf*) and *mtphantastica* (*mtphan*) mutants, which are impaired in a WUSCHEL-like homeobox (WOX) gene and the *ASYMMETRIC LEAVES1/ROUGH SHEATH2/PHANTASTICA* (*ARP*) MYB gene functions, respectively (Tadege *et al.*, 2011; Ge *et al.*, 2014). The *stf* and *mtphan* mutants have narrow blades with wider interspaces between leaflets and curl leaflets with longer rachises respectively, but both bear normal pulvini and exhibit nyctinastic movements (Figs 4e–h, S10, S11). The generated double mutants *mtdwf4a-1 stf* and *mtdwf4a-1 mtphan* both could completely close their leaflets at night (Figs 4e, S10). Statistical analyses of angles between LLs revealed that nyctinastic leaf movements of these two double mutants were nearly identical to that of the WT plants (Fig. 4h). Pulvinus-length measurements showed that the loss-of-function mutation of *MtDWF4A* was responsible for the shortened pulvinus, but no significant difference was found between *mtdwf4a* and these double mutant combinations (Figs 1h, S11). Furthermore, the structure and cell morphology of the pulvinus appeared to be relatively normal in both single mutants (*mtdwf4a*, *stf* or *mtphan*) and double mutants (*mtdwf4a stf* or *mtdwf4a mtphan*) when compared to WT (Figs 1i,m, 4f,g). These data collectively indicate that the *stf* and *mtphan* mutants had little role in effecting the pulvinus size and structure in the double mutants, suggesting

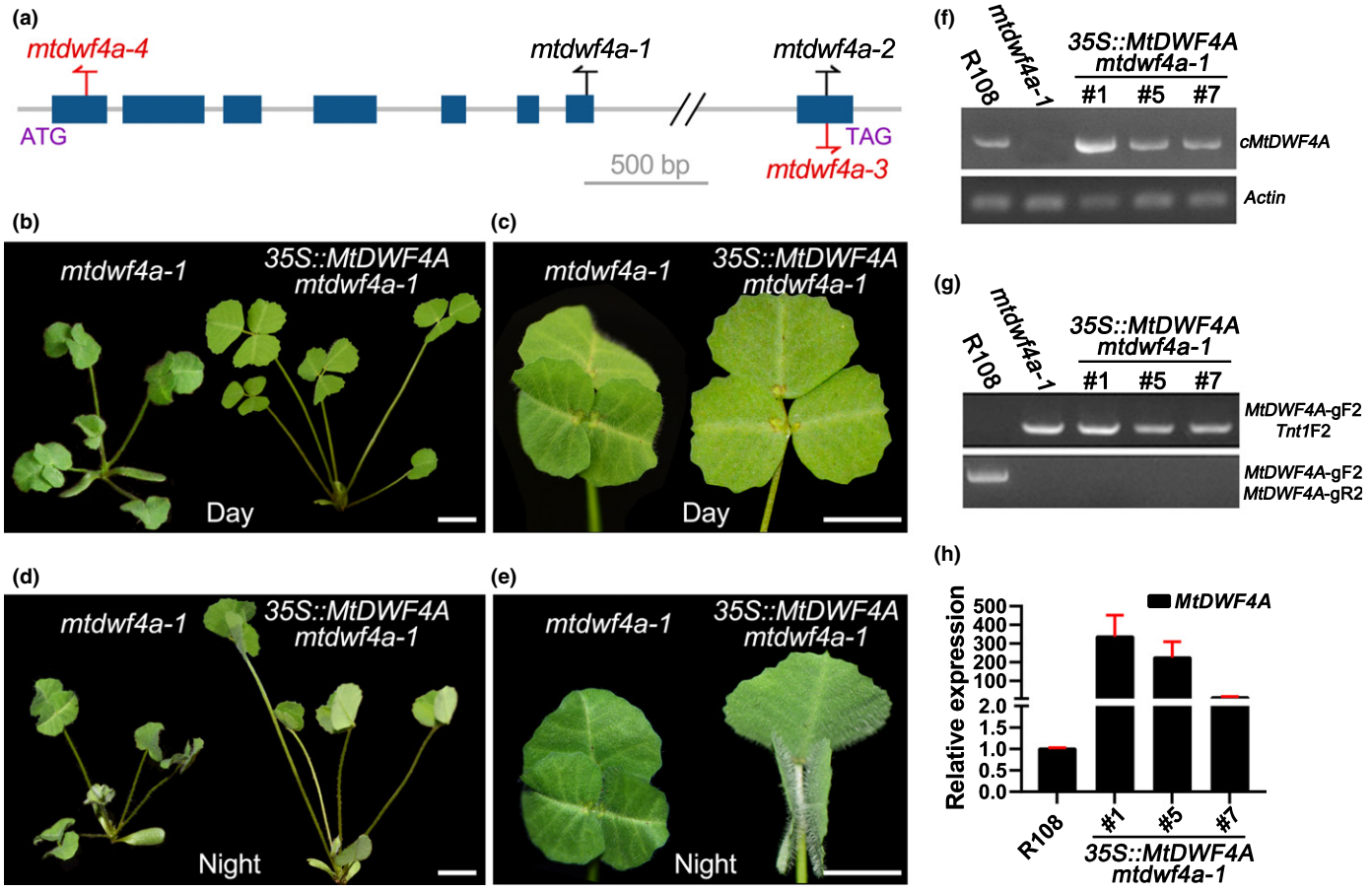

Fig. 2 Molecular cloning of *MtDWF4A* and the genetic complementation in *Medicago truncatula*. (a) The gene structure of *MtDWF4A* and *Tnt1* insertion sites of different alleles. The start codon (ATG) and stop codon (TGA) are indicated. Boxes represent exons and lines represent introns. (b–e) Genetic complementation of *mtdwf4a-1*. (b, d) Shown are the *mtdwf4a-1* mutant (left) and a representative *mtdwf4a-1* mutant transformed with *35S::MtDWF4A* (right) during daytime (b) and nighttime (d); (c, e) a close-up view of a compound leaf from (b) and (d), respectively (bars, 1 cm). (f) RT-PCR amplification of *MtDWF4A* from the wild-type (WT) and three independent *35S::MtDWF4A/mtdwf4a-1* (#1, #5, #7) transgenic lines. *M. truncatula ACTIN* gene was used as a loading control. (g) Genotyping PCR analysis of *MtDWF4A* in WT, the *mtdwf4a-1* mutant and *35S::MtDWF4A/mtdwf4a-1* transgenic lines. *MtDWF4A*-gF2/*MtDWF4A*-gR2 is a pair of specific primers for *MtDWF4A* genomic sequence. *Tnt1*F2 is a retrotransposon *Tnt1* specific primer. Positions of these primers in the *MtDWF4A* genome are presented in Supporting Information Fig. S3(a). (h) RT-qPCR analysis of expression level of *MtDWF4A* in leaves of WT and three independent *35S::MtDWF4A/mtdwf4a-1* transgenic lines. Expression of *MtDWF4A* was normalized with the *M. truncatula ACTIN* gene. Data are mean ± SD ($n = 3$ technical replicates); similar results were obtained in three biological replicates.

that the physical alterations of the leaf geometry but not the pulvinus identity in the double mutants led to the recovery of leaf movement. By contrast, the *elp1* mutation which changed the pulvinus into a petiole-like structure, was fully epistatic to the *mtdwf4a* mutation in the determination of the pulvinus identity (Fig. 4i). These results indicate that, distinct from the *ELP1* regulation of leaf movement by determining the pulvinus development, *MtDWF4A* appears to be very important to the leaf movement mainly because of its critical role in defining the compound leaf geometry.

Discussion

Several factors have been reported to influence the nyctinastic leaf movement process. The orthologs of *ELP1* have been demonstrated to determine the identity of the pulvinus among legumes (Chen *et al.*, 2012; Zhou *et al.*, 2012), and *GmIPLA1* was shown to regulate the pulvinus development in soybean (Gao *et al.*, 2017). Precise ion signal transmissions, K^+ and Cl^- channels and aquaporin are thought to regulate volume of the pulvinus motor cells and thus determine leaf movement (Moshelion *et al.*, 2002a,b; Oikawa *et al.*, 2018). Moreover, leaf movement is an energy-consuming process, and this rhythmic movement cannot be performed if the energy supply is blocked (Hermann, 1983). In this study, we found that mutation of *MtDWF4A* leads to loss of leaf movement capability. Considering previous studies, we firstly investigated if this is associated with pulvinus development but found that the *mtdwf4a* pulvinus presented intact organ identity and WT-like anatomical structure (Fig. 1j–m) without significant developmental deficiency except the length being shortened. We then conducted surgical experiments by mechanical ablation of the overlapping portions between leaflets and genetic crosses with multiple leaf mutants. Interestingly, the tailored leaflets of *mtdwf4a* could close at night (Fig. 4a–d), while leaves of *mtdwf4a stf* and

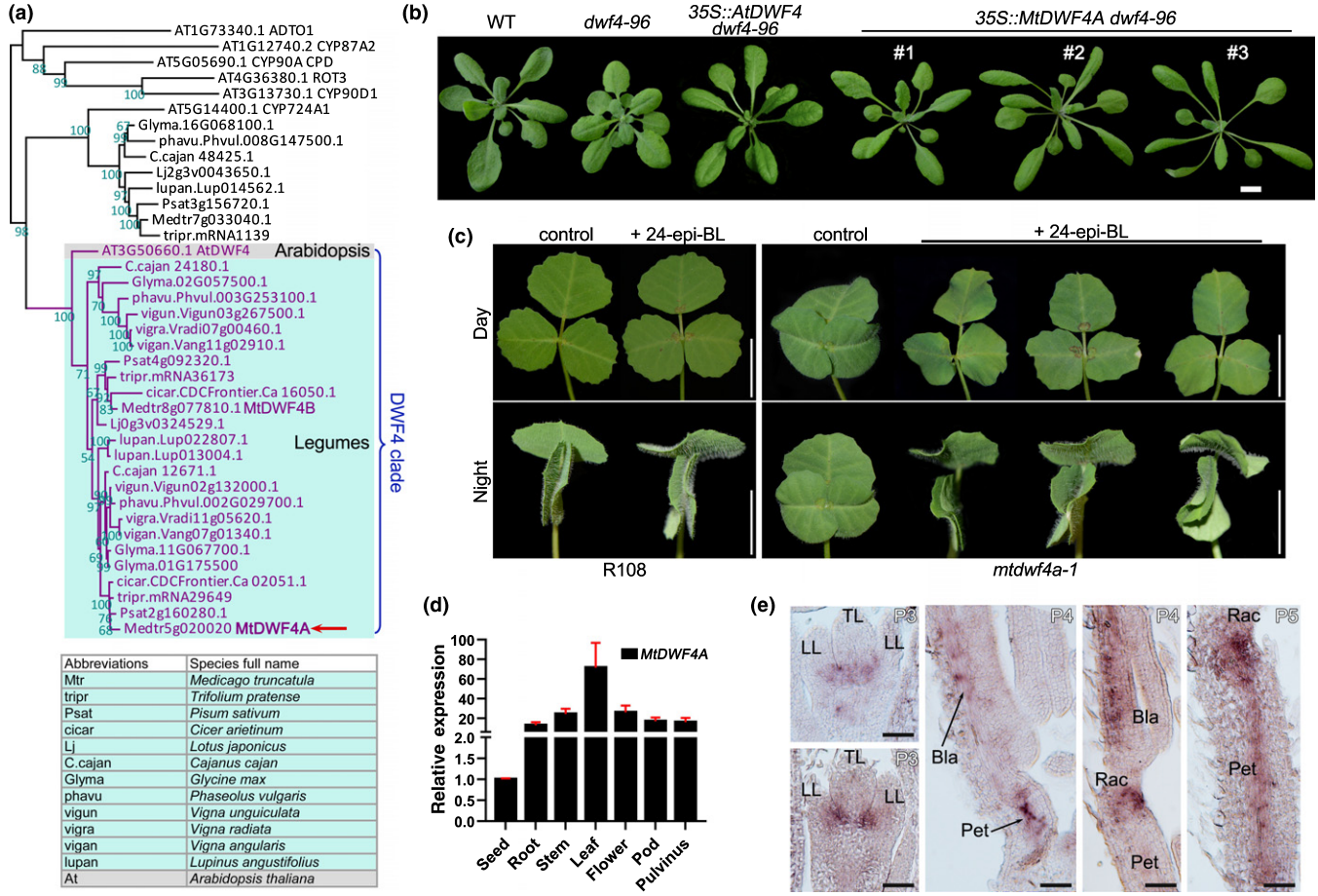

Fig. 3 Phylogenetic analysis and the expression pattern of *MtDWF4A*. (a) Maximum likelihood tree of MtDWF4A and its homologs from some legumes and *Arabidopsis*. All legume species and legume sequence names are light blue boxed. (b) Overexpression of *AtDWF4* and heterologous *MtDWF4A* can overcome the defect of *dwf4-96* mutant of *Arabidopsis thaliana* (bar, 1 cm). (c) Brassinolide (BL) feeding fully restored the compound leaf movement capability of the *mtdwf4a-1* mutant of *Medicago truncatula*. One-week-old plants grown in soil were sprayed by 1 μM of 24-epi-BL or control solution once a day for 2 wk and compound leaves of the third internode beneath the shoot apex were photographed at 10 d after the spraying stopped. (d) The relative expression level of *MtDWF4A* in different tissues in *M. truncatula*. Data are mean ± SD ($n = 3$ technical replicates); similar results were obtained in three biological replicates. (e) RNA *in situ* hybridization of *MtDWF4A* in leaf primordia at different developmental stages in *M. truncatula* (bars, 50 μm). Signals were detected in basal regions between LL and TL of the P3 leaf primordium, and the blade, rachis, and petiole regions of the P4 and P5 leaf primordium. P, plastochron; TL, terminal leaflet; LL, lateral leaflet; Bla, blade; Pet, petiole; Rac, rachis.

mtdwf4a mtphan double mutants exhibited normal nyctinastic movement as in WT leaves (Figs 4e–h, S10). It is reasonable to believe that the intrinsic mechanism of nyctinastic leaf movement of *mtdwf4a* is not significantly affected, and its inability to exhibit leaflet movement is mainly a consequence of the reduced spaces between leaflets, which causes a physical constraint on the movement. These provide us with a novel insight into the nyctinastic leaf movement, that the proper geometry of compound leaf is important for leaflets to close in the night, and shedding light on the importance of open space for organ movements in plants.

BRs, a group of steroid phytohormones, function at low concentrations and without long-distance transport, playing indispensable roles throughout plant growth and development (Clouse & Sasse, 1998). Plants with deficiency in BR biosynthesis or signaling pathway display characteristic pleiotropic phenotypes, including a dwarfed stature with darker green and epinastic round leaves, short petioles, reduced apical dominance, male sterility, and de-etiolation in the dark (Chory *et al.*, 1991; Li & Chory, 1997; Azpiroz *et al.*, 1998; Choe *et al.*, 1998; Cheng *et al.*, 2017). In the BR biosynthetic pathway, the cytochrome P450 (CYP90B1) encoded by the *DWF4* gene, mediates multiple 22 α-hydroxylation steps in *Arabidopsis* (Choe *et al.*, 1998). In this study, the *mtdwf4a* mutant exhibits mild BR-deficient phenotypes, including semi-dwarfism, short petioles and rachis, but normal fertility. This is significantly distinct from the typical BR-deficient *Arabidopsis dwf4* and *M. truncatula brassinosteroid-insensitive1* (*mtbri1*, BR receptor mutant) mutants that show severe dwarfism and sterility (Azpiroz *et al.*, 1998; Cheng *et al.*, 2017). Given that *MtDWF4A* has a highly homologous copy designated as *MtDWF4B*, it will be critical to explore the possibilities of functional redundancy and diversification between *MtDWF4A* and *MtDWF4B* in the BR biosynthetic pathways.

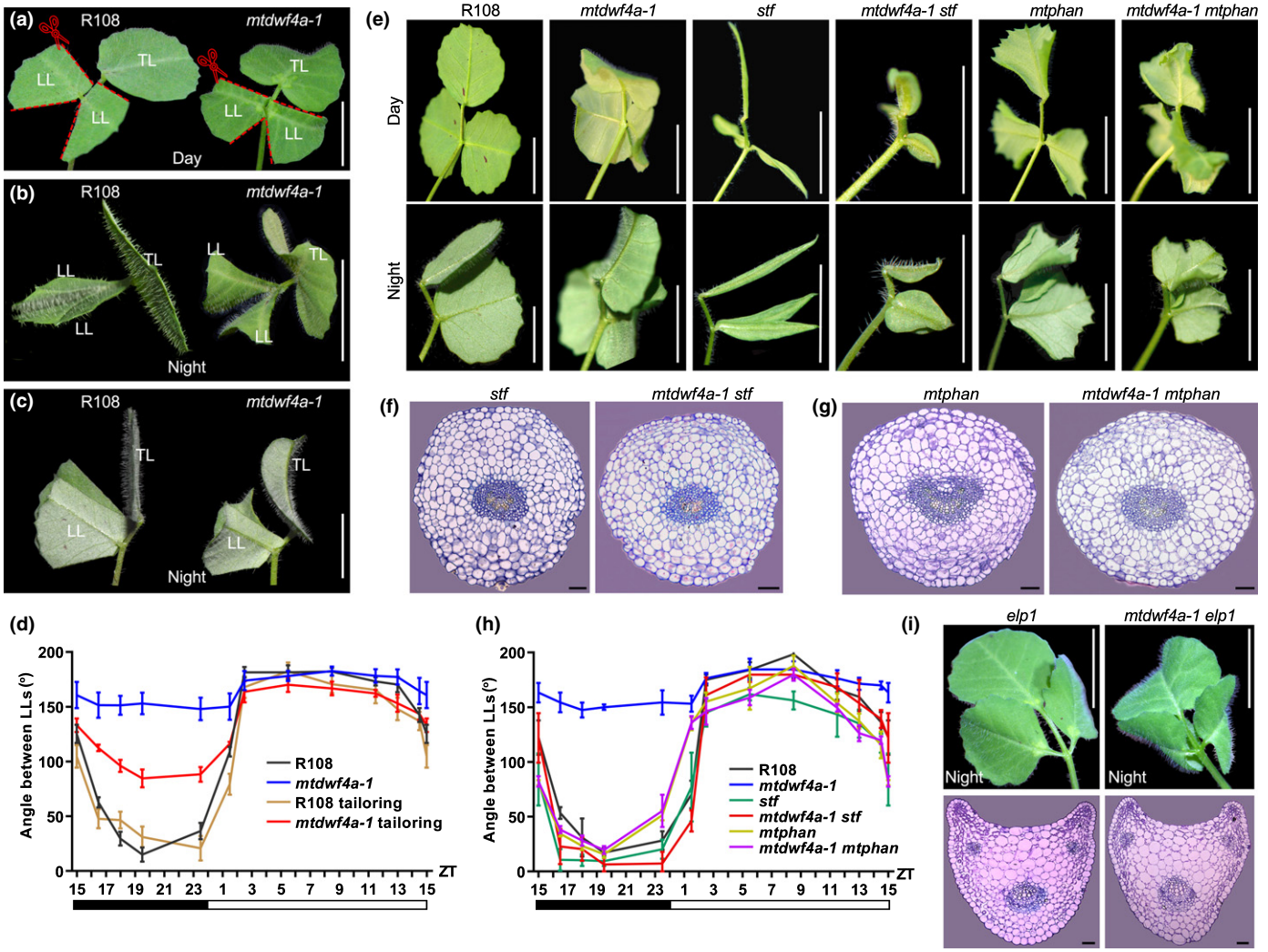

Fig. 4 Surgical experiments and genetic interactions in *Medicago truncatula*. (a–c) The tailored compound leaves of 1-month-old wild type (WT) (left) and *mtdwf4a-1* (right) during daytime (a) and nighttime (b, c). Third internode leaves beneath the shoot apex were selected and imaged at 2 d after tailoring. The removing regions are indicated by red dotted lines with scissors (bars, 1 cm). (d) Statistical analysis of angles between lateral leaflets (LLs) of the untreated and tailored leaves of 1-month-old WT and *mtdwf4a-1*. Black and white bars at the bottom indicate periods of dark and light, respectively. ZT, zeitgeber time. Values shown in the form mean ± SD ($n = 5$). (e) Genetic interactions between *mtdwf4a* and leaf-geometry mutants. The movement phenotypes of compound leaves from WT, *mtdwf4a-1*, *stf*, *mtdwf4a-1 stf* double mutant, *mtphan* and *mtdwf4a-1 mtphan* double mutant (left to right) (bars, 1 cm). (f–g) Semi-thin transverse sections of the terminal leaflet (TL) pulvinus of *stf, mtdwf4a-1 stf* double mutant, *mtphan* and *mtdwf4a-1 mtphan* double mutant (bars, 50 μm). (h) Statistical analysis of angles between LLs of WT, *mtdwf4a-1*, *stf*, *mtdwf4a-1 stf* double mutant, *mtphan* and *mtdwf4a-1 mtphan* double mutant. Values shown in the form mean ± SD ($n = 5$). (i) Genetic interaction between *mtdwf4a-1* and *elp1*. Upper planes: compound leaves from 1-month-old *elp1* (left) and *mtdwf4a-1 elp1* plants (right) during nighttime (bar, 1 cm). Bottom planes: semi-thin transverse section of the TL pulvinus of *elp1* (left) and *mtdwf4a-1 elp1* (right) (bars, 50 μm).

BR accumulation may play an important role in the pulvinus development of *M. truncatula* for the following reasons. First, the length of pulvinus in the *mtdwf4a* mutant background was reduced, which was evident by the comparisons between WT vs *mtdwf4a*, *stf* vs *mtdwf4a stf* and *mtphan* vs *mtdwf4a mtphan* (Figs 1h, S11). This is consistent with the function of BR to promote organ elongation (Choe *et al.*, 2001). Second, the complete removal of the overlapping parts of leaflets partially restored the movement phenotype of *mtdwf4a* compound leaves (Fig. 4d), indicating another mechanism involved MtDWF4A may work in parallel to regulate the leaf movement behavior besides its role in defining the compound leaf geometry. Most likely, MtDWF4A would act through the BR-signaling pathway to regulate the pulvinus development, and it is important to explore in future how the BRs affect the pulvinus function. Third, the pulvinus identity gene *ELP1* is homologous to the *Arabidopsis LOB* gene, which directly up-regulates the BR metabolic gene *phyB Activation-tagged Suppressor1-dominant* (*BAS1*) (Bell *et al.*, 2012; Gendron *et al.*, 2012), and overexpression of *ELP1* led to highly reduced petioles and rachises, distorted leaf blades and dwarfed status, to certain extent, similar to the phenotypes of the *mtdwf4a* mutants (Chen *et al.*, 2012), indicating a possible role of ELP1 in BR accumulation. However, analysis of *mtdwf4a elp1* double mutants revealed a fully epistatic interaction between *elp1* and

mtdwf4a in the pulvinus development (Fig. 4i), suggesting that the pulvinus identity determination is dependent on the function of ELP1 but not MtDWF4A. In view of these findings, we believe that it is of great significance in future to investigate how the temporal and spatial patterning of BR accumulation is involved in pulvinus development and what role ELP1 takes in this process.

Acknowledgements

The authors thank Kyle Warwick Tomlinson (Xishuangbanna Tropical Botanical Garden, Chinese Academy of Sciences (CAS), Kunming, China) for his critical reading and correcting of the manuscript, and Zhijia Gu and Wei Chang (Kunming Institute of Botany, CAS) for the SEM technical support and semi-thin sections respectively. The authors thank Wuhan Greensword Creation Technology Co. Ltd and Yunnan Tailangxuan Science & Technology Co. Ltd for their kind help. The authors also thank the Noble Research Institute (Ardmore, OK, USA) for providing the *Tnt1* mutants of *M. truncatula*. This study was supported by several National Natural Science Foundation of China (grant nos. U1702234, 31471171, 31700244), 'One Hundred Talent Project of the Chinese Academy of Sciences', 'High-end Scientific and Technological Talents in Yunnan Province', 'the Core Botanical Gardens, Chinese Academy of Sciences (CAS-CBG)', the Strategic Priority Research Program of the Chinese Academy of Sciences (XDB27030106 and XDA27030301), the Natural Science Foundation of Yunnan Province of China (2015, 2018FB033), the West Light Foundation of the Chinese Academy of Sciences, the Youth Innovation Promotion Association CAS (to BZ) and the Special Research Assistant Program CAS (to LH).

Author contributions

JC designed the research; WZ performed most experiments; LH carried out phylogenetic analysis; CW participated in semi-thin sections; LH and YeL performed RNA *in situ* hybridization experiments; TY and YuL participated in genetic cross experiments; MT contributed new reagent/analytic tools; WZ, LH, QW, HH and SD analyzed the data; LH and JC wrote and revised the manuscript with imput from WZ, who wrote the first draft. QB, BZ and MT provided help and advice, and corrected the manuscript.

ORCID

Jianghua Chen https://orcid.org/0000-0003-0715-1859
Liangliang He https://orcid.org/0000-0002-2169-4326
Million Tadege https://orcid.org/0000-0002-3306-3695
Chaoqun Wang https://orcid.org/0000-0002-1544-3125
Baolin Zhao https://orcid.org/0000-0001-9573-4178

References

Azpiroz R, Wu Y, LoCascio JC, Feldmann KAJTPC. 1998. An Arabidopsis brassinosteroid-dependent mutant is blocked in cell elongation. *Plant Cell* **10**: 219–230.

Bajguz A, Chmur M, Gruszka D. 2020. Comprehensive overview of the Brassinosteroid biosynthesis pathways: substrates, products, inhibitors, and connections. *Frontiers in Plant Science* **11**: 1034.

Bell EM, Lin W-C, Husbands AY, Yu L, Jaganatha V, Jablonska B, Mangeon A, Neff MM, Girke T. 2012. *Arabidopsis* LATERAL ORGAN BOUNDARIES negatively regulates brassinosteroid accumulation to limit growth in organ boundaries. *Proceedings of the National Academy of Sciences, USA* **109**: 21146–21151.

Chabaud M, Ratet P, Araújo SdS, Duque ASRLA, Harrison M, Barker DG. 2007. Agrobacterium tumefaciens-mediated transformation and *in vitro* plant regeneration of *Medicago truncatula*. In: Mathesius U, Journet EP, Sumner LW, eds. *The* Medicago truncatula *handbook*. [WWW document] URL http://www.noble.org/MedicagoHandbook/.

Chen J, Moreau C, Liu Y, Kawaguchi M, Hofer J, Ellis N, Chen R. 2012. Conserved genetic determinant of motor organ identity in *Medicago truncatula* and related legumes. *Proceedings of the National Academy of Sciences, USA* **109**: 11723–11728.

Chen J, Yu J, Ge L, Wang H, Berbel A, Liu Y, Chen Y, Li G, Tadege M, Wen J *et al.* 2010. Control of dissected leaf morphology by a Cys(2)His(2) zinc finger transcription factor in the model legume *Medicago truncatula*. *Proceedings of the National Academy of Sciences, USA* **107**: 10754–10759.

Cheng X, Gou X, Yin H, Mysore KS, Li J, Wen J. 2017. Functional characterisation of brassinosteroid receptor *MtBRI1* in *Medicago truncatula*. *Scientific Reports* **7**: 9327.

Choe S, Dilkes BP, Fujioka S, Takatsuto S, Sakurai A, Feldmann KAJTPC. 1998. The *DWF4* gene of Arabidopsis encodes a cytochrome P450 that mediates multiple 22α-hydroxylation steps in brassinosteroid biosynthesis. *Plant Cell* **10**: 231–243.

Choe S, Fujioka S, Noguchi T, Takatsuto S, Yoshida S, Feldmann KAJTPJ. 2001. Overexpression of *DWARF4* in the brassinosteroid biosynthetic pathway results in increased vegetative growth and seed yield in *Arabidopsis*. *The Plant Journal* **26**: 573–582.

Chory J, Nagpal P, Peto CA. 1991. Phenotypic and genetic analysis of *det2*, a new mutant that affects light-regulated seedling development in *Arabidopsis*. *Plant Cell* **3**: 445–459.

Clough SJ, Bent AF. 1998. Floral dip: a simplified method for *Agrobacterium*-mediated transformation of *Arabidopsis thaliana*. *The Plant Journal* **16**: 735–743.

Clouse SD, Sasse JM. 1998. Brassinosteroids: essential regulators of plant growth and development. *Annual Review of Plant Biology* **49**: 427–451.

Coen ES, Romero JM, Doyle S, Elliott R, Murphy G, Carpenter R. 1990. floricaula: a homeotic gene required for flower development in *Antirrhinum majus*. *Cell* **63**: 1311–1322.

Cote GG. 1995. Signal transduction in leaf movement. *Plant Physiology* **109**: 729.

Darwin C, Darwin F. 1881. *The power of movement in plants*. New York, NY, USA: D. Appleton & Co.

d'Erfurth I, Cosson V, Eschstruth A, Lucas H, Kondorosi A, Ratet PJTPJ. 2003. Efficient transposition of the *Tnt1* tobacco retrotransposon in the model legume *Medicago truncatula*. *The Plant Journal* **34**: 95–106.

Ding J, Mao L, Wang S, Yuan B, Feng Y. 2013. Determination of endogenous brassinosteroids in plant tissues using solid-phase extraction with double layered cartridge followed by high-performance liquid chromatography-tandem mass spectrometry. *Phytochemical Analysis* **24**: 386–394.

Du J, Zhao B, Sun X, Sun M, Zhang D, Zhang S, Yang W. 2016. Identification and characterization of multiple intermediate alleles of the key genes regulating Brassinosteroid biosynthesis pathways. *Frontiers in Plant Science* **7**: 1893.

Feder N, Obrien TP. 1968. Plant microtechnique: some principles and new methods. *American Journal of Botany* **55**: 123–142.

Gao J, Yang S, Cheng W, Fu Y, Leng J, Yuan X, Jiang N, Ma J, Feng X. 2017. GmILPA1, encoding an APC8-like protein, controls leaf petiole angle in soybean. *Plant Physiology* **174**: 1167–1176.

Ge L, Peng J, Berbel A, Madueno F, Chen R. 2014. Regulation of compound leaf development by *PHANTASTICA* in *Medicago truncatula*. *Plant Physiology* **164**: 216–228.

Gendron JM, Liu J-S, Fan M, Bai M-Y, Wenkel S, Springer PS, Barton MK, Wang ZY. 2012. Brassinosteroids regulate organ boundary formation in the shoot apical meristem of *Arabidopsis*. *Proceedings of the National Academy of Sciences, USA* **109**: 21152–21157.

Gorton HL, Satter RL. 1984. Extensor and flexor protoplasts from *Samanea* pulvini. *Plant Physiology* **76**: 685–690.

Harvey DM. 1979. *Evaluation of an apulvinic foliar mutation in* P. sativum. Seventieth Annual Report. Norwich, UK: John Innes Institute, p 34.
He L, Liu Y, He H, Liu Y, Qi J, Zhang X, Li Y, Mao Y, Zhou S, Zheng X *et al.* 2020. A molecular framework underlying the compound leaf pattern of *Medicago truncatula*. *Nature Plants* **6**: 511–521.
Hermann S. 1983. Turgorins, hormones of the endogeneous daily rhythms of higher organized plants—detection, isolation, structure, synthesis, and activity. *Angewandte Chemie International Edition in English* **22**: 695–710.
Jiang C, Chen C, Huang Z, Liu R, Verdier J. 2015. ITIS, a bioinformatics tool for accurate identification of transposon insertion sites using next-generation sequencing data. *BMC Bioinformatics* **16**: 72.
Kawaguchi M. 2003. *SLEEPLESS*, a gene conferring nyctinastic movement in legume. *Journal of Plant Research* **116**: 151–154.
Kong Y, Han L, Liu X, Wang H, Wen L, Yu X, Xu X, Kong F, Fu C, Mysore KS *et al.* 2020. The nodulation and nyctinastic leaf movement is orchestrated by clock gene LHY in *Medicago truncatula*. *Journal of Integrative Plant Biology* **62**: 1880–1895.
Li J, Chory JJC. 1997. A putative leucine-rich repeat receptor kinase involved in brassinosteroid signal transduction. *Cell* **90**: 929–938.
Moshelion M, Becker D, Biela A, Uehlein N, Hedrich R, Otto B, Levi H, Moran N, Kaldenhoff R. 2002a. Plasma membrane aquaporins in the motor cells of *Samanea saman*: diurnal and circadian regulation. *Plant Cell* **14**: 727–739.
Moshelion M, Becker D, Czempinski K, Mueller-Roeber B, Attali B, Hedrich R, Moran N. 2002b. Diurnal and circadian regulation of putative potassium channels in a leaf moving organ. *Plant Physiology* **128**: 634–642.
Oikawa T, Ishimaru Y, Munemasa S, Takeuchi Y, Washiyama K, Hamamoto S, Yoshikawa N, Mutara Y, Uozumi N, Ueda M. 2018. Ion channels regulate nyctinastic leaf opening in *Samanea saman*. *Current Biology* **28**: 2230–2238.
Racusen R, Satter RL. 1975. Rhythmic and phytochrome-regulated changes in transmembrane potential in *Samanea pulvini*. *Nature* **255**: 408–410.
Runions A, Tsiantis M, Prusinkiewicz P. 2017. A common developmental program can produce diverse leaf shapes. *New Phytologist* **216**: 401–418.
Satter RL, Galston AWJS. 1971. Potassium flux: a common feature of Albizzia leaflet movement controlled by phytochrome or endogenous rhythm. *Science* **174**: 518–520.
Scarpella E, Barkoulas M, Tsiantis M. 2010. Control of leaf and vein development by auxin. *Cold Spring Harbor Perspectives in Biology* **2**: a001511.
Tadege M, Lin H, Bedair M, Berbel A, Wen J, Rojas CM, Niu L, Tang Y, Sumner LW, Ratet PJTPC. 2011. *STENOFOLIA* regulates blade outgrowth and leaf vascular patterning in *Medicago truncatula* and *Nicotiana sylvestris*. *Plant Cell* **23**: 2125–2142.
Tadege M, Wen J, He J, Tu H, Kwak Y, Eschstruth A, Cayrel A, Endre G, Zhao PX, Chabaud M *et al.* 2008. Large-scale insertional mutagenesis using the *Tnt1* retrotransposon in the model legume *Medicago truncatula*. *The Plant Journal* **54**: 335–347.
Tamura K, Dudley J, Nei M, Kumar S. 2007. MEGA4: Molecular evolutionary genetics analysis (MEGA) software version 4.0. *Molecular Biology and Evolution* **24**: 1596–1599.
Thompson JD, Gibson TJ, Plewniak F, Jeanmougin F, Higgins DG. 1997. The CLUSTAL_X windows interface: flexible strategies for multiple sequence alignment aided by quality analysis tools. *Nucleic Acids Research* **25**: 4876–4882.
Ueda M, Ishimaru Y, Takeuchi Y, Muraoka Y. 2019. Plant nyctinasty – who will decode the 'Rosetta Stone'? *New Phytologist* **223**: 107–112.
Wang H, Chen J, Wen J, Tadege M, Li G, Liu Y, Mysore KS, Ratet P, Chen R. 2008. Control of compound leaf development by *FLORICAULA/LEAFY* ortholog *SINGLE LEAFLET1* in *Medicago truncatula*. *Plant Physiology* **146**: 1759–1772.
Wang ZY, Seto H, Fujioka S, Yoshida S, Chory J. 2001. BRI1 is a critical component of a plasma-membrane receptor for plant steroids. *Nature* **411**: 219.
Young ND, Debelle F, Oldroyd GE, Geurts R, Cannon SB, Udvardi MK, Benedito VA, Mayer KF, Gouzy J, Schoof H *et al.* 2012. The *Medicago* genome provides insight into the evolution of rhizobial symbioses. *Nature* **480**: 520–524.
Zhao B, He L, Jiang C, Liu Y, He H, Bai Q, Zhou S, Zheng X, Wen J, Mysore KS *et al.* 2020. *Lateral Leaflet Suppression 1* (*LLS1*), encoding the MtYUCCA1 protein, regulates lateral leaflet development in *Medicago truncatula*. *New Phytologist* **227**: 613–628.
Zheng X, He L, Liu Y, Mao Y, Wang C, Zhao B, Li Y, He H, Guo S, Zhang L *et al.* 2020. A study of male fertility control in *Medicago truncatula* uncovers an evolutionarily conserved recruitment of two tapetal bHLH subfamilies in plant sexual reproduction. *New Phytologist* **228**: 1115–1133.
Zhou C, Han L, Fu C, Chai M, Zhang W, Li G, Tang Y, Wang ZY. 2012. Identification and characterization of *petiolule-like* pulvinus mutants with abolished nyctinastic leaf movement in the model legume *Medicago truncatula*. *New Phytologist* **196**: 92–100.

Supporting Information

Additional Supporting Information may be found online in the Supporting Information section at the end of the article.

Fig. S1 Allelism test of NF9200 and NF11207 mutants.

Fig. S2 Expression profiles of the candidate genes.

Fig. S3 Segregation analysis of the candidate gene.

Fig. S4 Phenotypes of *mtdwf4a* alleles in daytime and nighttime.

Fig. S5 Protein sequence of MtDWF4A was conserved in *Medicago truncatula*.

Fig. S6 RT-PCR and PCR analysis of the *Arabidopsis thaliana* transgenic plants.

Fig. S7 Quantitative analyses of BR content of WT and *mtdwf4a-1* shoot apical tissues.

Fig. S8 The removing of TL or distal portions of LLs failed to restore the *mtdwf4a-1* movement phenotype.

Fig. S9 Both the first unifoliate leaf and the remaining TL part of compound leaf after tailoring could incline to the petiole during nighttime in the *mtdwf4a-1* mutant.

Fig. S10 Genetic interactions between *mtdwf4a-1* and leaf geometry mutants.

Fig. S11 The pulvinus length of single and double mutants.

Table S1 List of primer sequences.

Table S2 Seven homozygous *Tnt1* insertion sites in *mtdwf4a-1* from re-sequencing results.

Table S3 Mutant alleles and the insertions sites.

Please note: Wiley Blackwell are not responsible for the content or functionality of any Supporting Information supplied by the authors. Any queries (other than missing material) should be directed to the *New Phytologist* Central Office.